Werk

Jahr: 1981
Kollektion: fid.geo
Signatur: 8 Z NAT 2148:50
Digitalisiert: Niedersächsische Staats- und Universitätsbibliothek Göttingen
Werk Id: PPN1015067948_0050
PURL: http://resolver.sub.uni-goettingen.de/purl?PPN1015067948_0050

LOG Id: LOG_0030
LOG Titel: Acceleration processes at the earth's bow shock
LOG Typ: article

Übergeordnetes Werk

Werk Id: PPN1015067948
PURL: http://resolver.sub.uni-goettingen.de/purl?PPN1015067948
OPAC: http://opac.sub.uni-goettingen.de/DB=1/PPN?PPN=1015067948

Contact

Niedersächsische Staats- und Universitätsbibliothek Göttingen
Georg-August-Universität Göttingen
Platz der Göttinger Sieben 1
37073 Göttingen
Germany
Email: gdz@sub.uni-goettingen.de

J Geophys (1981) 50: 114–122

Journal of Geophysics

Acceleration Processes at the Earth's Bow Shock *

V. Formisano[1], S. Orsini[2]
[1] Space Science Department, ESA-ESTEC, Noordwijk, The Netherlands
[2] Laboratorio Plasma Spazio, CNR-Frascati, Italy

Abstract. ISEE-2 solar wind data are used to study acceleration processes at the Earth's bow shock by looking at the details of particle velocity distribution functions on several crossings. In the magnetosheath the transmitted accelerated particles show, downstream of a quasi-perpendicular shock, energy spectra which are different from those observed downstream of quasi-parallel shocks. A clear cut-off in the energy spectrum can be identified in the first case, while pronounced high energy tails are observed in the second case. The reflected backstreaming particles also show a cut-off in the energy spectrum. We conclude that the same acceleration mechanism generates the transmitted accelerated particles and the reflected ions. This mechanism is located at the shock, and is due to the electric field component tangent to the shock. Some evidence for weaker acceleration can be found at quasi-parallel shocks, where 5–10 keV ion flux appears to be constant going from upstream to downstream-zones. We conclude that diffuse ions cannot be accelerated at the shock, but are the result of this interaction of reflected particles with the solar wind. Particles which are stationary in the shock frame have been observed for both quasi-parallel and quasi-perpendicular shocks.

Key words: Collisionless shocks – Acceleration at shocks – Earth's bow shock – Shock structure

Introduction

Particles accelerated and reflected at the Earth's bow shock interact with the solar wind in the foreshock region. (Fairfield 1969; Asbridge et al. 1968). The acceleration at the shock was modelled by Sonnerup (1969) and by Greenstadt (1975); evidence for ion acceleration at the shock was reported by Montgomery et al. (1970) and by Formisano and Hedgecock (1973a). The presence of a high energy tail, downstream of the quasi-perpendicular turbulent shocks observed by Formisano and Hedgecock (1973b) (see also the review by Formisano, 1977) is also an indication that strong acceleration takes place at the Earth's bow shock. A fraction of the particles accelerated at the shock escape upstream and interact with the solar wind. Recently a division into two groups has been suggested for this population of accelerated particles: "reflected" and "diffuse" accelerated particles, characterized by different angular-energy distribution, the first being a population of cold particles, localised in energy and angle; the second being a population of hot particles and appearing "diffuse" in energy and angle (Gosling et al. 1978). Only diffuse backstreaming particles are observed simultaneously with the magnetohydrodynamic (MHD) magnetosonic waves (Paschmann et al. 1979; Bonifazi et al. 1980). Formisano et al. (1980) have shown how the solar wind proton bulk speed and direction of flow oscillate when diffuse particles are observed, and how the solar wind is paractically uperturbed in the presence of reflected particles. Formisano and Amata (1976) and Bame et al. (1980) have shown that the solar wind slows down and deviates from its direction while interacting with the diffuse particles.

Although there is evidence for acceleration at the bow shock, a detailed experimental study of this process is not yet available in the literature and the relationship between the reflected particles and shock structure is not clear. Are the diffuse and reflected particles coming from the same region of the shock or from different regions? Are the diffuse particles produced by the interaction of the reflected particles with the solar wind or accelerated at the shock they produce the instabilities and associated waves, by interseting with the solar wind?

It is likely that the same mechanism that is accelerating particles to produce "reflected" ions can also produce transmitted accelerated particles. So another interesting question is: what are the properties of the transmitted accelerated particles? Can they reach the same energy as the reflected particles?

In the following we will address some of these problems by analyzing plasma particle data from the solar wind plasma experiment on board ISEE-2. The experiment has been described by Bonifazi et al. (1978); here we mention only that for hot particle populations (such as magnetosheath, backstreaming particles and occasionally also the solar wind) we can increase the time resolution of the measurements from 96 s per sample to 12 s per sample because the 64 energy windows available were obtained by means of 8 fast scans of the energy range covered (55 eV–11 keV). Each of these 8 subcycles provides 8 energy windows with complete angular distribution. Therefore, for a population of hot particles they provide enough information to characterize plasma parameters.

In this paper we first present a qualitative study of some properties of the reflected and transmitted accelerated particles in order to identify their energy properties. We than study in detail two shock crossings where reflected particles are observed immediately upstream and two shock crossings where diffuse particles are observed immediately upstream. Conclusions and discussions will be presented at the end of the paper.

* Paper presented at the Workshop on Acceleration of Particles by Shock Waves, 7–9 October 1980, Max-Planck-Institut für Aeronomie, Lindau, Federal Republic of Germany

0340-62X/81/0050/0114/$01.80

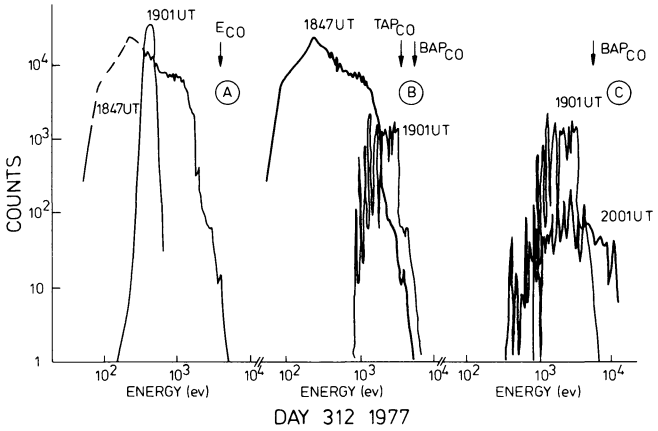

Fig. 1. Comparison of ion energy spectra for day 312, 1977. *A* Solar wind (1901 UT) and magnetosheath (1847 UT): transmitted accelerated ions are observed in the magnetosheath above solar wind energies. *B* Magnetosheath (1847 UT) and solar wind reflected particles (1901 UT): these particles can reach energies higher than those of the transmitted ones. *C* Reflected ions (1901 UT) and diffuse particles (2001 UT): the diffuse particles can have energies higher than reflected particles

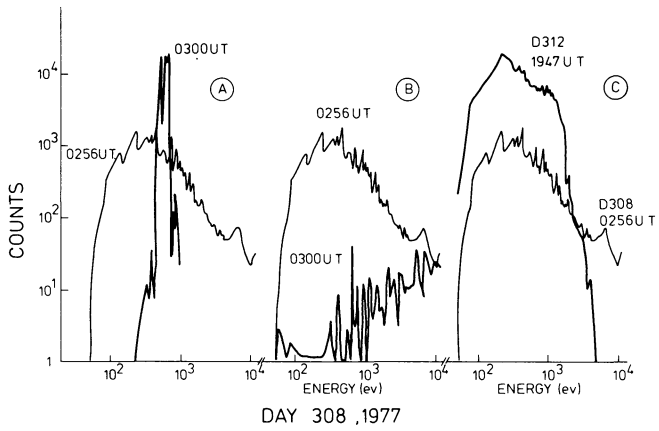

Fig. 2. Comparison of ion energy spectra for day 308, 1977. *A* Solar wind (0300 UT) and magnetosheath (0256 UT). *B* Magnetosheath (0256 UT) and solar wind diffuse ions (0300 UT). *C* Magnetosheath downstream of quasi-perpendicular shock (day 312, 1947 UT) and downstream of quasi-parallel shock (day 308, 0256 UT)

Energy Spectra of Particle Populations near the Bow Shock

A first qualitative answer to some of the problems mentioned above can be obtained by means of a simple inspection of measured energy spectra in the bow shock region. Energy spectra observed in the vicinity of the bow shock, when reflected particles are present, are displayed in Fig. 1. Data refer to day 312, 1977, when the bow shock was crossed at 1,857 UT (Fig. 8 and Paschmann et al. 1979). The solar wind peak energy was found to be near 500 eV, and very few particles had energy above 600 eV (Fig. 1a). In the magnetosheath the energy spectrum is observed to extend to much higher energies, and a cut-off was actually observed at 3,850 eV. (The cut-off was located by identifying the energy where the count rate went below 3 ct/s.) The acceleration mechanism for the transmitted particles is, in this case, not able to provide many particles with energy larger than 3,850 eV. Reflected particles were observed in the solar wind, and their energy spectrum is compared with that of transmitted ions in Fig. 1b. A cut-off is also observed for the reflected ions, but in this case it is at 5,400 eV, i.e. at an energy level 1,500 eV higher. The particles that are able to escape upstream gain more energy than the ones transmitted downstream. One hour later the solar wind energy is still the same, but the magnetic field direction has changed slightly in such a way that MHD waves and diffuse particles are observed. A comparison with the reflected particles is presented in Fig. 1c: The diffuse ions are spread over a wider range of energies and do not show any cut-off. The important point we would like to stress here is that the spectrum of the diffuse population shows many particles with energy higher than the solar wind energy, higher than the energy of transmitted ions and higher than the reflected ion energy. It is also interesting to look at magnetosheath energy spectra downstream of a quasi-parallel shock. A typical case is shown in Fig. 2 for day 308, 1977. Solar wind protons were observed at 0300 UT, to have energy around 700 eV (Fig. 2a). In the magnetosheath, at 0256 UT, the energy spectrum had a shape different from that of day 312, 1847 UT: no cut-off was observed, and at 10 keV the flux was at least a factor 50 larger on day 308 than on day 312 although the total number density was lower. There may be fewer transmitted accelerated ions in the quasi-parallel shock, but they reach energies higher than downstream of a quasi-perpendicular shock (Fig. 2c). The magnetosheath energy spectrum in Fig. 2a actually has the shape of a power law: $E^{-3.8}$. The previous result is confirmed by looking at more than 100 magnetosheath passes. If we compare transmitted and reflected ion energy spectra for day 308 (Fig. 2b), we see that at high energies the flux is comparable inside and outside the shock. This is to be expected if the diffuse ions are the result of the interaction of the reflected ions with the solar wind. Conversely if the shock is the source, it must produce as many diffuse as transmitted ions for quasi-parallel conditions, which is different from what is observed in a quasi-perpendicular shock. In any case we are dealing with two acceleration mechanisms. As we shall see later we have evidence that the quasi-parallel shock is not producing the diffuse ions, although it is accelerating particles to lower energies than a quasi-perpendicular shock.

The cut-off energy (E_{co}) for the transmitted ions downstream of quasi-perpendicular shocks has been statistically studied in order to infer properties of the acceleration mechanisms. E_{co} has a very strong dependence on the energy of the solar wind (E_{sw}). In Fig. 3 we show a scatter plot of E_{co} versus E_{sw} with the best linear fit given by $E_{co}=10.6\,E_{sw}-1{,}519$ eV, the correlation coefficient being 0.92. The three highest points in Fig. 3 are only lower limits because we observe within our energy range (up to 11 keV) only part of the decrease of the energy spectrum and, from extrapolation, 10 counts should be reached above 15 keV. We have also studied the scatter of the points present in Fig. 3 using the linear fit given above to bring the observed E_{co} to a fixed solar wind energy ($E_{sw}=500$ eV). The cut-off energy for fixed energy input (E_{co}, $E_{sw}=500$ eV) is shown to be correlated with the magnetosonic Mach number (M_{MS}) in Fig. 4 with correlation coefficient 0.49. Larger M_{MS} values occur together with lower E_{co} when E_{sw} is fixed. This result may be important when we extrapolate from the bow shock to astrophysical shocks, in order to obtain large acceleration factors. This needs to be further investigated in view of the low correlation coefficient found.

In order to study properties of acceleration processes at the shock, we note first that reflected ions have not been observed

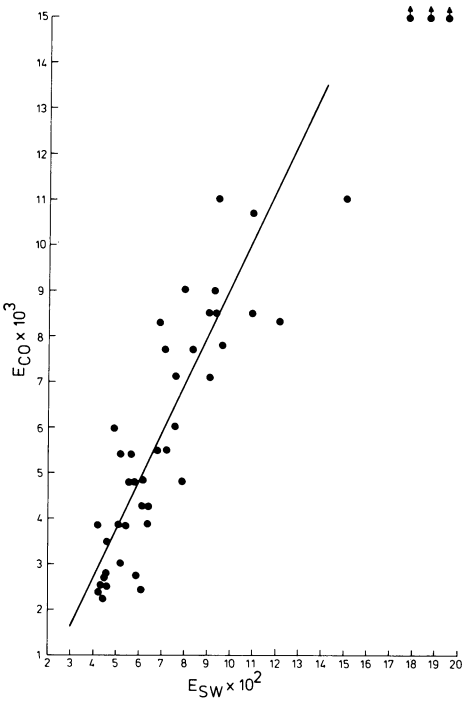

Fig. 3. Relationship between the cut-off energy (E_{co}) of the transmitted particles with the solar wind energy E_{sw}. The linear best fit through the points is given by $E_{co}=10.6\ E_{sw}-1{,}519$

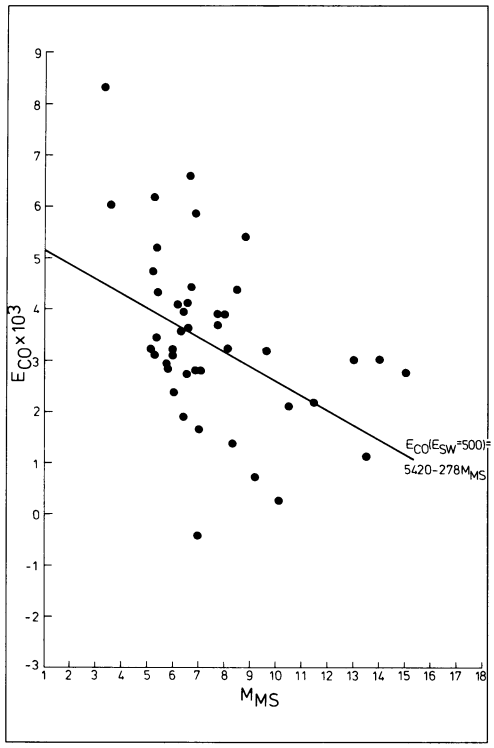

Fig. 4. Relationship between E_{co} of transmitted particles normalized to a fixed solar wind energy ($E_{sw}=500$ eV), and the Mach number M_{MS}. The best linear fit through the points is also given.

upstream of shocks with $\widehat{B\bar{n}} \geqq 70°$, while diffuse ions have not been observed upstream of shocks with $\widehat{B\bar{n}} \geqq 60° \sim 55°$ (Bonifazi and Moreno 1981). It is clearly of interest to study particle properties at shocks with $\widehat{B\bar{n}} > 70°$, $55° < \widehat{B\bar{n}} < 70°$ and $\widehat{B\bar{n}} < 55°$ in order to locate the source of the reflected and transmitted ions, and in order to identify the acceleration mechanism.

Quasi-Perpendicular Shocks

One shock crossing with $\widehat{B\bar{n}} = 78°$, and no backstreaming particles, was observed on day 335, 1977 at 2220 UT. Data for the period 2216–2222 UT are shown in Fig. 5. This figure deserves some comment because figures of this type will be used several times later. The angular distribution of one or two energy channels is shown at the top, for the solar wind proton peak and, if present, for the peak in the energy spectrum of the reflected ions. In the magnetosheath usually only one energy channel is shown, namely the peak in the energy spectrum. At the shock one or two significant energy channels are shown depending on the relevance of the information to be presented. Numbers like $E21$ indicate that the angular distribution of energy channel number 21 is shown. It should be noted that in the angular distribution there is a blind sector at all energies (Bonifazi et al. 1978) with no measurement between $-34°$ and $-56°$ indicated by a dashed sector in the figures. The angular distributions are always presented with the sun direction given by the arrow on the top of the figure. The radial distance from the centre gives, on a logarithmic scale, the particles counted when the instrument was looking in that direction. For the 90° sectors the number of particles counted has been divided by 16 in order to have measurements comparable with the 5.6° sectors, and should be considered as the average counts over 16 sectors 5.6° wide. Below the angular distributions there is, in Fig. 5, a strip showing energy spectra. Each energy spectrum is shown on a log scale, however the energy scale is shown in a large size when more than 8 energy channels are presented. It should be noted that the energy range covered is the same in both cases. The subcycle spectra (8 channels) are used in order to increase our time resolution without shrinking the energy range covered. One or two energy spectra are shown for each subcycle, taken looking in two different directions. The energy spectrum observed in the solar wind direction is represented by a dashed line, the one at 90° to it (or magnetosheath direction, 90° wide) is represented by a continuous line. Magnetic field data (one component B_z or the magnitude B) is shown at the bottom of the figure in order to locate the spacecraft with respect to the shock. The timing of the energy spectra is shown by open boxes. The parameters M_{MS}, $\widehat{B\bar{n}}$ and β characterising the shock are shown on the left hand side of the magnetic field strip, and were computed using the solar wind hourly averages published by King (1980).

The shock observed on day 335 at 2220 UT was a quasi-perpendicular turbulent shock. In the solar wind (spectrum 1) a typical situation was observed with no backstreaming particles. The solar wind energy spectrum shows the multiple peaks due to $^4He^{2+}$ and heavy ions as is usually observed with electrostatic analyzer. The angular distribution also shows the cold collimated solar wind ion beam. As we move close to the shock (spectrum 2) we also observe, together with the solar wind, a consistent population of particles that gyrate around $\bar{B}$ and are able to go upstream for a distance $\simeq 1\ R_j$ (gyroradius) (foot of the shock). Note that the energy spectrum of these reflected particle peaks at energies below the solar wind energy. The next spectrum is very interesting: we are still on the solar wind side of the shock, as it is confirmed by the cold beam revealed by the angular distribution. The solar wind has, however, been slowed down considerably: the peak is observed in channel 13

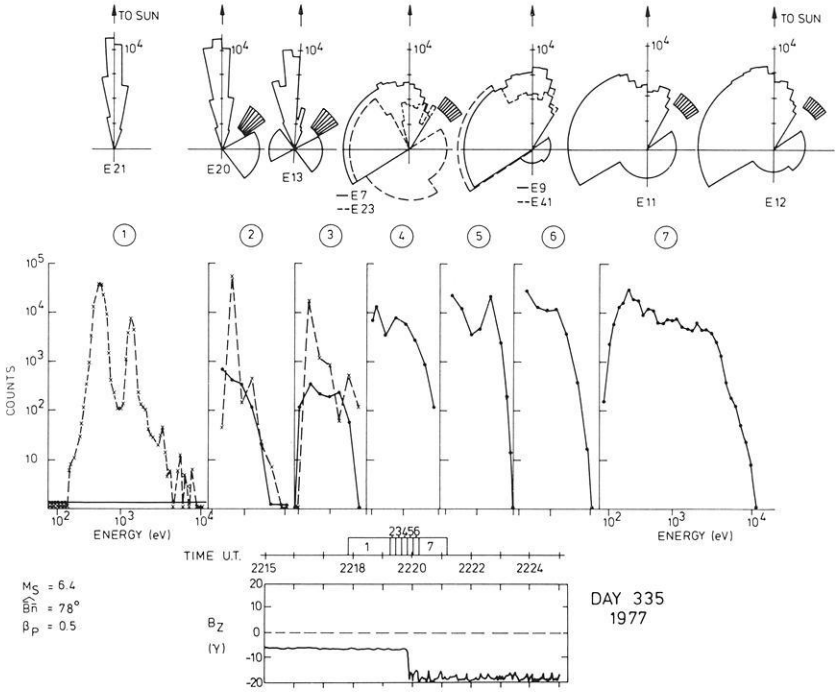

Fig. 5. Details of a quasi-perpendicular shock crossing with no reflected ions. On the top strip we have angular information for the peak proton energy channel. Two angular distributions (two energies indicated by energy channel number) are shown when two peaks (two particle populations) are observed. Note the "blind" sector at $-34°$ to $-56°$, where no measurements are taken for technical reasons. On the middle strip we have energy spectra covering the energy range 55 eV–11 keV. Note that the energy scale is reduced when only 8 energy channels (subcycles) are used. On the *bottom* of the figure the shock parameters (magnetosonic Mach number, $\widehat{B\bar{n}}$ and β_p) are given on the *left hand side*; also, on the *bottom* of the figure, the time scale is given with indication of the time intervals during which the observed numbered spectra were taken. Note in this figure the increase of the cut-off energy from 3.5 keV (spectrum 2) to 3.6 (3), 5.5 (5), 6.5 (6), 8 kev (7). See text for further explanations

(442 eV) while before it was in channel 20 (641 eV). From the angular distribution it can be seen that the solar wind has already been somewhat deflected and heated. At the same time, at the high energy end of the observed spectrum, the flux has increased to almost the magnetosheath level. In the spetrum observed at 90° to the solar wind there is evidence for a first peak at 442 eV and for a second peak at 1,606 eV. The presence of the two peaks is confirmed by the next two energy spectra (4 and 5 in Fig 5) which clearly show magnetosheath plasma already heated (see the angular distributions). The first peak is at 236 eV and the second at 800–1,000 eV in spectrum 4 and around 2,000 eV in spectrum 5. The second peak becomes a plateau in spectrum 6 and a long high energy tail followed by a cut-off at ~8,000 eV in spectrum 7.

The cut-off was always present in the spectra at 90° to the solar wind direction (full lines in Fig. 5) and is found at lower energies in spectra 2 and 3 when no particles are observed at energies of 3,500 and 3,650 eV, while in spectrum 5 it is at 5,500, and in spectrum 7 at 8,000 eV. It is evident that the particles accelerated at the shock are not able to escape upstream in this situation ($\widehat{B\bar{n}} = 78°$). Only transmitted accelerated particles are observed, and their maximum energy increases going from upstream to downstream. A typical feature for this kind of shock is a bimodal ion velocity distribution immediately after the shock and just upstream of it. Both accelerated and decelerated particles are able to reach the immediate upstream region (foot) of the shock before being convected downstream.

Next we will deal with quasi-perpendicular shock structures with reflected particles observed upstream. Two cases with different solar wind energies will be described in order to be able to explore energies much larger (day 312, 1977) or lower (day 337, 1977) than those associated with the solar wind. On day 312, 1978 the bow shock was crossed at 1852:50 UT (Fig. 6), with $\widehat{B\bar{n}} = 60°$ and $M_{MS} = 4$. Due to rather low magnetic field intensity and high plasma density, the value of β (plasma pressure to magnetic pressure ratio) was rather high for this shock crossing: $\beta = 19$ (see also Russell and Greenstadt 1979). The high value of β increases the magnetic turbulence as discussed by Formisano et al. (1976). Here we are interested in the behaviour of the plasma particles. In Fig. 6 the solar wind energy spectrum is shown on the right side (dashed curve), as this was an outbound crossing. Upstream reflected ions are observed between 0.8 and 8 keV together with the cold solar wind (angular distribution of the spectrum taken at 1900 UT). Some fluctuations are present in both the solar wind and the reflected particle energy spectrum (see also the data for this crossing in the previous section). The magnetosheath energy spectrum is shown on the left hand side and is similar to the sheath spectrum 7 in Fig. 5. The cut-off energy is observed at 3,850 eV. Spectra 2 and 3, on the magnetosheath side of the shock, revealed the presence of two peaks, one at low energy and another at 1,100 eV. Spectrum 4 is very interesting for its shape and for the low energy angular distribution. In channel 9 (350 eV) the angular distribution shows two peaks, one being the cold solar wind, the other one being similar to the magnetosheath population of particles. At higher energy a peak is observed only in this direction. This peak is at 1 keV like the peak observed in the magnetosheath. Spectrum 4 identifies the shock in the ion plasma particles as it separates magnetosheath from cold solar wind energy spectra. The cut-off of the second peak, which is going to generate the reflected ions is at 5,370 eV (as it is also confirmed by spectrum 5). Spectrum 4 is observed between the first large pulse in the magnetic field intensity and the second final increase of intensity of $\bar{B}$. The solar wind is observed from spectrum 5 to spectrum 9 together with reflected ions. We note a decrease of the peak flux intensity of the reflected ions between spectra 5 and 8, and this decrease corresponds also to a change of the peak energy from 1 keV to 2 keV. At the same time, however, the cut-off does not change and is still at 5,400 eV. We conclude therefore that between spectra 5 and 8 there is no further acceleration, and the difference in the reflected ion spectrum can be explained by loss of the low energy part of the population. This conclusion is confirmed by a direct comparison (overlapping) of spectra 8 and 5: at high energy the two spectra overlap,

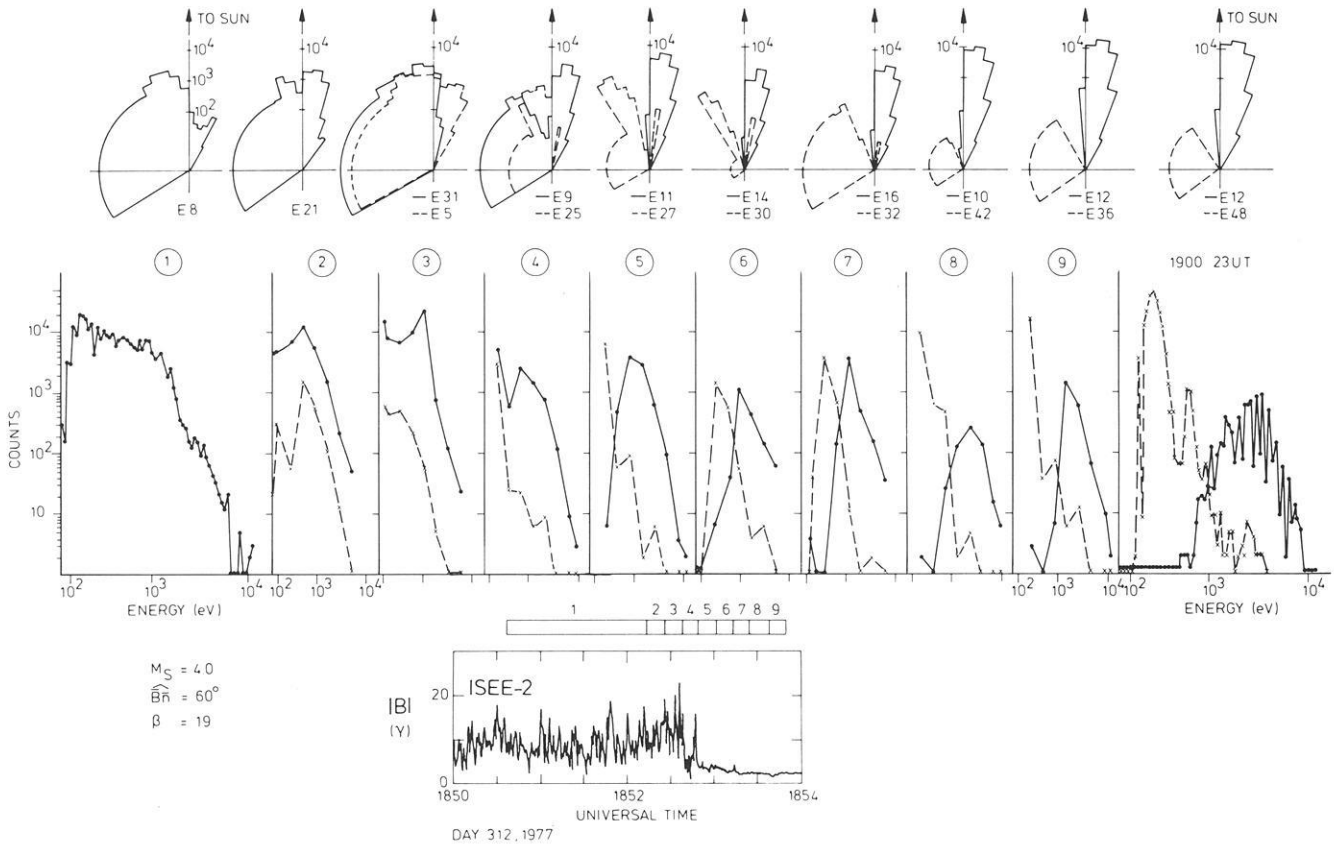

Fig. 6. Details of quasi-perpendicular shock crossing with reflected ions observed upstream (day 312, 1977, 1853 UT). Note the decrease of flux intensity and related increase of peak energy between spectrum 5 and spectrum 8 of the reflected ions (*continuous lines*). The format of the figure is the same as in Fig. 5; the magnetic field intensity from ISEE-2 is shown on the bottom. Note the two streams in the angular distribution (4) identifying the shock crossing

while at low energy part of the population present in 5 is missing in 8.

In conclusion we locate the acceleration region, by means of spectra 4 and 5, at the large magnetic intensity gradients, i.e. at the shock, because on the solar wind side the flux of reflected ions decreases as we move away from the shock, and on the sheath side the flux observed in the second peak (accelerated particles) also decreases going away from the shock.

The behaviour of the reflected ions at low energy is studied by means of the observations on day 337, 1977, when the bow shock was crossed at 0055 UT. Our data are shown in Fig. 7 together with one component (B_z) of the magnetic field data from the ISEE-1 spececraft. As the magnetic field is shown just as a guide to locate the observations with respect to the shock, the complete magnetic information from the spacecraft ISEE-2 (from which the plasma data were obtained) is not needed. The shock was again a quasi-perpendicular shock with $\widehat{B\vec{n}} = 69°$ and $M_{MS}=4.5$, $\beta_p=0.1$. Reflected ions were observed in spectrum 1, showing a cut-off similar to the one already presented in Fig. 1 b. The magnetosheath spectrum shows the same features we have seen for the previous two shocks (see spectrum 10 in Fig. 7). From spectra 2–9 in Fig. 7 we can study how the reflected ion energy spectrum changes at low energies (below the solar wind energy) when we approach the bow shock from upstream. From spectrum 1 we see that no backstreaming particles were observed below the solar wind energy (1,200 eV at the peak). In the solar wind energy range some fluctuations of the reflected particles appear in spectrum 1. In spectra 2, 3 and 4 the reflected particle spectra show no fluctuations, but tell us rather that there are no reflected particles at energies below the solar wind energy. In this sense it is interesting to note in the angular distributions that in the solar wind peak energy channel no reflected particles are observed in spectra 1–4. In spectra 5–7 we see a modification of the reflected ion spectrum, in the sense that particles are now added at energies lower than the solar wind energy, and at very high energies. In spectra 8 and 9 we observe that the solar wind has been partially deflected and thermalized. From these spectra we conclude that we are at the shock, i.e. we see that at low energy we still have a cold population, while at high energy (the second peak in spectrum 9 is at 3,500 eV) the plasma is hot and appears from all directions. This mixed situation is observed for another complete cycle (now shown in the figure) before spectrum 10 is observed in the magnetosheath. Subcycles of these data not shown in the figure present bimodal energy spectra like spectrum 3 in Fig. 6.

In conclusion we have shown that quasi-perpendicular shocks do always accelerate particles. For $\widehat{B\vec{n}} > 70°$ the accelerated particles can only be transmitted, although they are already observed in the foot of the shock. For $\widehat{B\vec{n}} < 70°$ they can leave the shock, and are observed as reflected ions upstream of it. At the shock we have energy spectra with two peaks and angular distributions with two peaks. The transmitted particles always show a cut-off at an energy that depends on the solar wind velocity (see previous section). The backstreaming reflected particles also show a cut-off, but at an energy higher than the cut-off for the transmitted ones. For $\widehat{B\vec{n}} > 70°$ the cut-off of the transmitted particles moves

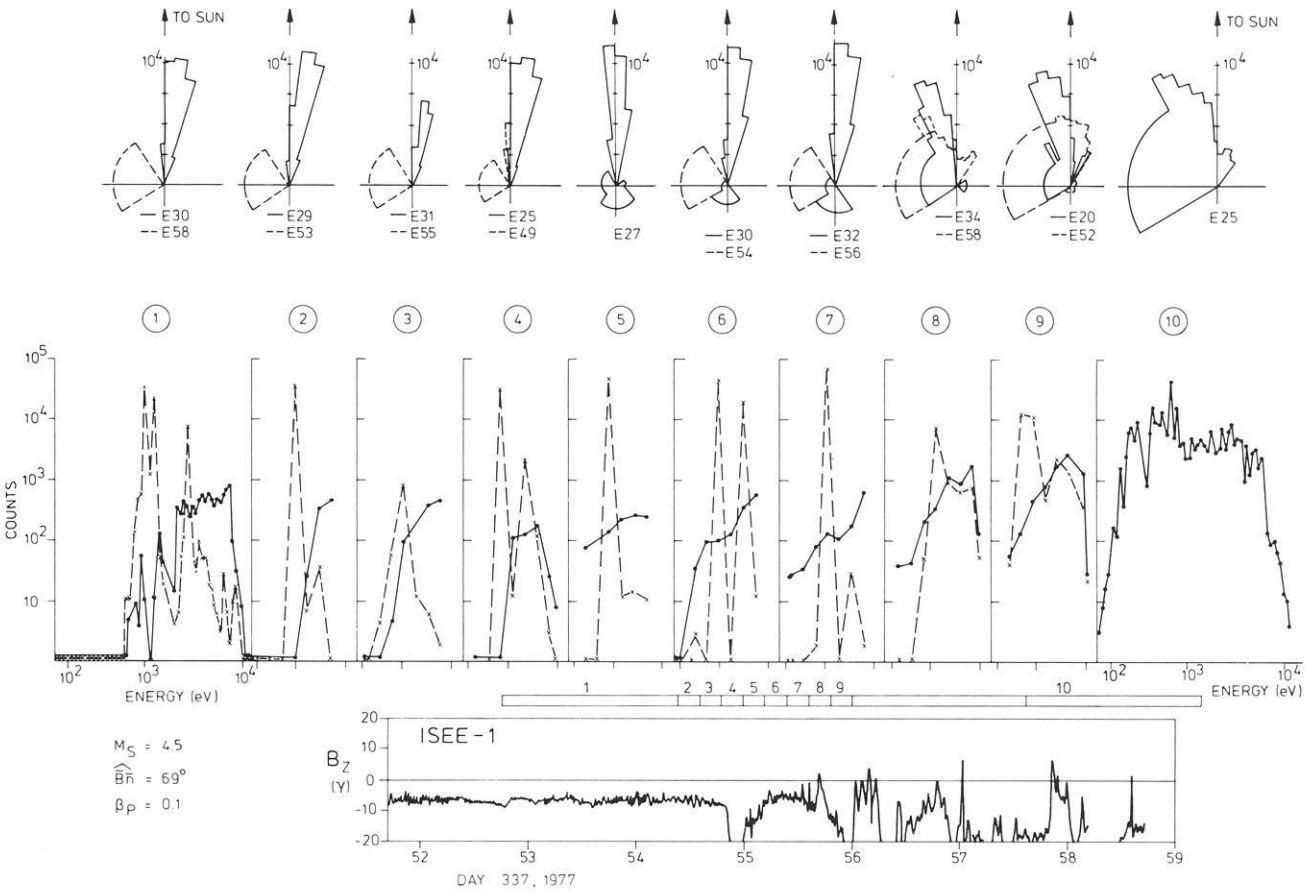

Fig. 7. Details of a quasi-perpendicular shock crossing with reflected particles observed upstream (day 337, 1977, 0055 UT). Note the increase of particles flux at energies below the solar wind energies as we approach the shock. On the bottom one component (B_z) of the magnetic field observed by ISEE-1 is shown as a reference. The format of the figure is the same as in Fig. 5

from lower to higher energies (from 3,500 eV to 8,000 eV) as we move from the foot of the shock to the sheath side of it. The flux intensity of the reflected ions increases as we move closer and closer to the shock. Close to the shock a population of low energy particles is added at energies lower than that associated with the solar wind. These particles are probably stationary in the shock frame, and may play an important role in the dissipation mechanism.

Quasi-Parallel Shocks

A quasi-parallel shock observed at 0259 UT on day 308, 1977 is shown in Fig. 8. As already mentioned, the upstream solar wind is very much perturbed when diffuse particles are observed, i.e. in front of quasi-parallel shock. Downstream of the shock there is no evidence for a cut-off in the proton energy spectrum and a long high energy tail is seen; fluxes of 10 keV particles comparable with the fluxes of 10 keV diffuse upstream ions are also observed (spectra 1 and 10 in Fig. 8). In Fig. 8, as we approach the shock from the magnetosheath side, the proton energy spectrum does not show the two peaks and the plateau observed in Fig. 5 (spectra 5 and 7), Fig. 6 (spectra 3 and 1), and Fig. 7 (spectra 9 and 10) for quasi-perpendicular shocks. Spectrum 4 in Fig. 8, which may be compared with spectrum 6 in Fig. 5, shows that the "plateau" due to transmitted particles, if present, has an ion flux a factor 20 lower than the first (main) peak. This plateau, on the other hand, can also be interpreted as the sum of the diffuse ions of upstream origin, plus ions locally (at the shock) accelerated and/or heated and/or scattered. We note that spectra (and angular distributions) 4 and 5 in Fig. 8 are rather "intermediate" between the cold solar wind and the hot magnetosheath: spectrum 5 shows a decelerated warm solar wind, while the angular distributions in 3 and 4 show that the plasma has not yet been deflected. The spectrum – angular distribution that identifies the shock (spectrum 6 in Fig. 8) is also the one that most resembles the quasi-perpendicular shock observations (spectrum 3 in Fig. 5 and spectrum 4 in Fig. 6). In the angular distribution two streams are observed and at 90° to the solar wind the energy spectrum shows accelerated particles. With respect to the solar wind, however, the acceleration at this shock is much smaller than at quasi-perpendicular shocks: the ratio E_{accel}/E_{sw} is 2.9 on day 335, 1977 (680 eV (solar wind) to 2,000 eV (transmitted particles, second peak)) and only 1.4 on day 308, 1977 (680 eV (solar wind) to 950 eV (accelerated particles) at the shock – spectrum 6). These accelerated particles are not seen downstream, while upstream of the shock we see (going from spectrum 6, to 7, 8, 9 and 10) that their flux decreases rapidly, until they are practically absent even upstream in spectrum 10. Our interpretation of this data is that the acceleration mechanism valid for quasi-perpendicular shocks, also works here (with $\widehat{Bn} = 30°$), although with much lower efficiency. In this case, the accelerated particles are quickly scattered in the phase space due to the presence of large amplitude waves carried at the shock by the solar wind itself. These waves have been produced by the interaction of the reflected particles with the solar wind far upstream of the shock. In this picture the diffuse ions,

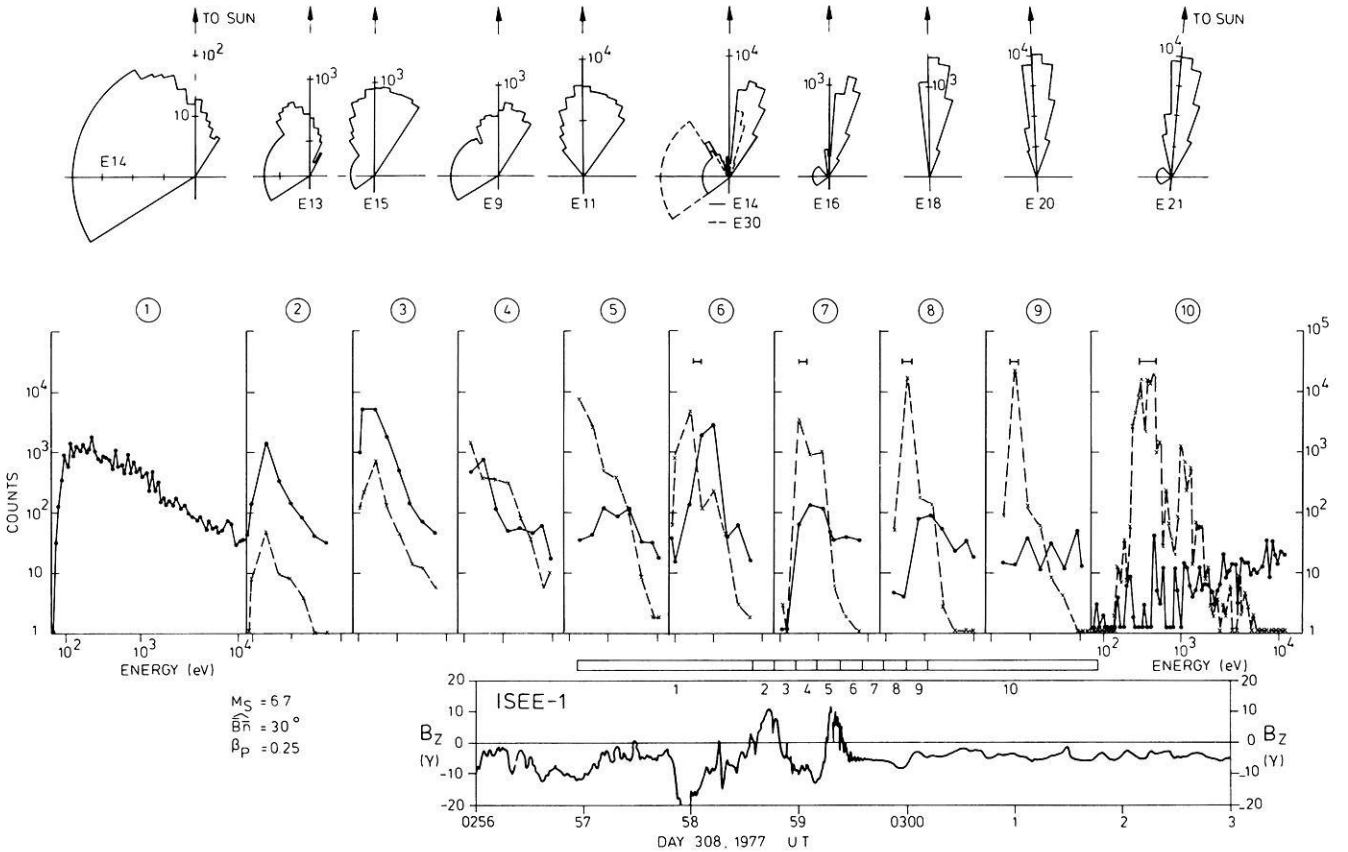

Fig. 8. Details of a quasi-parallel shock crossing with diffuse ions observed upstream (day 308, 1977, 0259 UT). The format of the figure is the same as in Fig. 5. Note the double ion streams in the angular distribution (6)

which show no clear direction of motion and a strongly oscillating angular distribution, (Formisano et al. 1980) are the results of some further acceleration mechanism due to wave particle interaction in the foreshock region.

This picture is confirmed by our second example of quasi-parallel shock crossing: day 316, 1977 at 1929 UT (Fig. 9). In this case $\widehat{B\bar{n}}$ is still smaller than in the previous case: $\widehat{B\bar{n}} = 24°$ and we find hardly any evidence for acceleration at the shock. Our data are shown in Fig. 9 for the period 1927–1931 UT when a quasi-crossing of the shock was observed. The last spectrum on the right hand side was observed after the shock was finally crossed at 1940 UT. Upstream of the shock large amplitude MHD waves are observed in the magnetic component B_z together with diffuse ions (spectra 1 and 2). Downstream of the shock (spectra 7, 8 and 9) again we find no evidence for either a second peak or a pleateau of transmitted particles. We do find, however, a long tail of energetic particles. with a power law-like energy spectrum. The shock is identified in spectrum 6 when the two population (solar wind and particles at 90° to it) reach similar fluxes, showing two beams in the angular distribution.

It is interesting to look at energy spectra 2–5. In spectrum 2 we have the same situation as in spectrum 1: solar wind plus diffuse ions at high energy. As we approach the shock the situation changes and we add a new population at low energies. Spectrum 3 shows that, at 90° to the solar wind, we observe an energy spectrum with two peaks: one below the solar wind energy at ≈ 100 eV and the second above 4 keV. The two populations are separated by a gap: no particles are observed between 1,200 and 1,800 eV. The low energy particles are probably stationary in the shock frame. Spectrum 4 shows that the flux of the low energy population has increased, and starts to fill the gap previously mentioned. The flux intensity of the high energy population, on the other hand, does not change. In spectrum 5 in the quadrant looking at the sun, the solar wind is deflected and slowed down, whereas at 90° to the solar wind a practically flat energy spectrum is observed between 50 eV and 10 keV. As on day 308, the energy spectrum observed at the shock (spectrum 6 in Figs. 8 and 9) is the only one that may perhaps give an indication of acceleration. This is, however, a rather weak indication, and the acceleration would be still smaller than for the case of Fig. 8.

In conclusion we may say that at quasi-parallel shocks there is less evidence (compared with quasi-perpendicular structures) for acceleration of particles. The acceleration is in any case smaller. Downstream of these shocks there is no evidence for a cut-off in the energy spectrum, i.e. no limit to the acceleration factor, and a long high energy tail (power law-like) is observed in ion energy spectra. When some small acceleration seems to be present at the shock, the accelerated particles are quickly scattered in phase space, so that no evidence of special features related to them is found immediately upstream or downstream of the shock. At very high energies (5–10 keV) the main feature observed is the continuity in the ion flux level from upstream, through the shock, downstream. Close to the shock a new population of particles is added, which is probably stationary in the shock frame of reference.

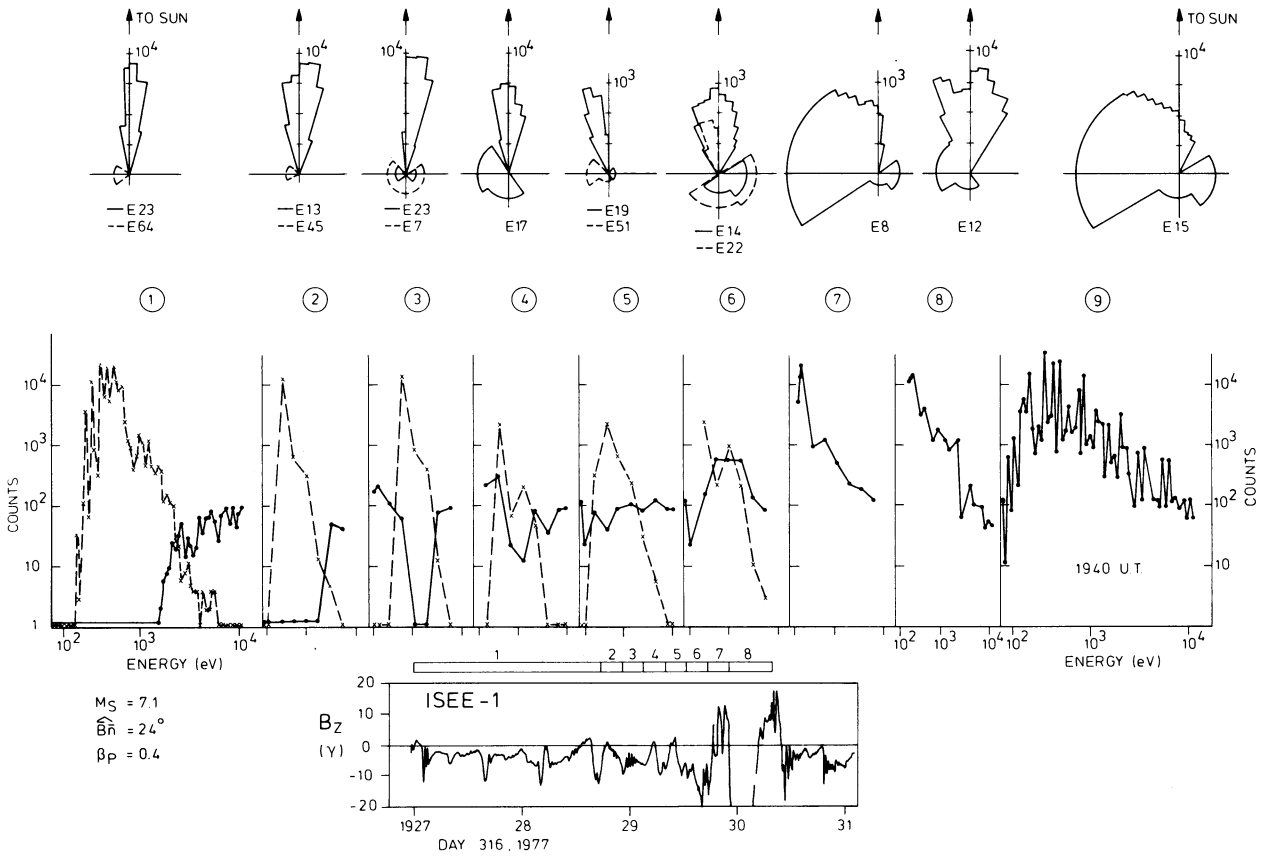

Fig. 9. Details of a quasi-parallel shock crossing with diffuse particles observed upstream (day 316, 1977, 1929 UT). The format of the figure is the same as in Fig. 8. Note the double ion streams in the angular distribution (6) and the low energy particles (stationary in the shock frame) in spectra 3 and 4

We interpret these observations as evidence for the bow shock being a source of decreasing power for reflections as $\widehat{B\vec{n}}$ changes from 90° to 0°. The ions leaving the shock in the region with $\widehat{B\vec{n}} < 70°$ interact with the solar wind at some distance from the shock, and generate all the MHD waves observed in the foreshock region. These waves also scatter the reflected ions in phase space, generating the diffuse particles which are then carried at the shock and downstream of it together with the waves. These diffuse ions are observed together with heated solar wind particles in the magnetosheath, where they give rise to the long, high energy tail.

Summary and Discussions

We have, in this study, presented a number of observations concerning the acceleration mechanisms present in the Earth's bow shock region. In summary it has been shown that:

a) Downstream of quasi-perpendicular shocks the transmitted particles do not show any cut-off in their energy spectrum, the maximum acceleration factor ranging between 5 and 11 times the solar wind energy.

b) Downstream of quasi-parallel shocks the transmitted particles do not show any cut-off in the energy spectrum, and few particles seem to have been accelerated to energies higher than downstream of quasi-perpendicular shocks (power law-like spectrum).

c) Upstream of the quasi-perpendicular shocks, the reflected ions also show a cut-off in the energy spectrum on the high energy side; this cut-off, however, is at higher energies than the one for the transmitted accelerated particles downstream of the same shock crossings.

d) The cut-off energy of the transmitted particles appears to move toward higher energies for increasing solar wind speed.

e) The cut-off energy of the transmitted particles decreases with increasing Mach number once the dependence on the solar wind velocity has been eliminated.

f) The 5–10 keV ion flux level is constant across quasi-parallel shocks.

g) A detailed study of quasi-perpendicular shocks with $\widehat{B\vec{n}} > 70°$ shows that

– acceleration is occurring at the shock as a bimodal energy spectrum is observed immediately downstream of it

– the accelerated particles cannot leave the shock on the upstream side (transmitted population)

– a two peaks angular distribution is observed at the shock

– the cut-off in the energy spectrum moves from "low" to high energies as we move from the foot of the shock to the magnetosheath

– at the shock, low energy particles are observed (pseudo trapped particles).

h) A detailed study of quasi-perpendicular shocks with $70° > \widehat{B\vec{n}} \geqq 60°$ shows the same characteristics listed in g), except that the accelerated particles can also leave the shock moving upstream (reflected backstreaming population). For these particles we note that

– the flux decreases as we move away from the shock

– the apparent increase in the average energy of the backstreaming accelerated ions as we move away from the shock

is due to loss of the low energy population as these particles are carried downstream by the solar wind.

i) A detailed study of the quasi-parallel shock crossings with diffuse ions upstream shows that some features of the quasi-perpendicular shocks are kept, such as the double-peaked angular distribution at the shock. We note, however, that

– the acceleration of particles at the shock, if present at all, is less effective

– evidence for these accelerated particles is quickly lost as we move away from the shock layer, probably because they are quickly scattered in the phase space

– way upstream of the shock there has to be another acceleration mechanism producing the diffuse ions, as these particles also have energies larger than the reflected ones and do not show any cut-off

– while at high energies (5–10 keV) the ion flux is constant, as we go from upstream through the shock downstream; at low energies, just upstream of the shock, a new population with energy comparable or even smaller than the solar wind energy is observed (pseudo trapped particles).

Concerning the problem of the origin of diffuse ions, we may say that there is enough evidence from the detailed study of crossings of quasi-parallel structures to show that they are not generated at the shock, unlike the reflected particles. On the other hand there are several indications that the diffuse ions are the result of the interaction between the reflected particles and the solar wind. The continuity of the ion flux with energy 5–10 keV across the shock exludes the shock itself as a source for these particles. The acceleration at quasi-parallel shocks is weaker, not stronger, than at quasi-perpendicular shocks, therefore these shocks cannot provide ions with energies larger than the energy of reflected ions. In our opinion the reflected particles do interact with the solar wind, but the interaction has a long growth time compared with the time the particles need to travel a few Earth radii. This may not be true if the unstable waves are already present, as it may be at quasi-parallel shocks with $\widehat{\mathbf{B}\mathbf{n}}$ not too small. In the interaction the reflected ions are scattered in phase space, therefore some of them will also be accelerated, and the resulting diffuse ions will be carried by the solar wind at the shock (where the newly generated population of reflected ions will be added to them and quickly scattered) and downstream (where they will form the long, high energy tail of the magnetosheath ion velocity distribution). Our data therefore support the interpretation of the solar wind reflected ions interaction given by Paschmann et al. (1979) and Bame et al. (1980) in contrast with the analysis by Greenstadt et al. (1980).

Concerning the problem of the acceleration mechanism, we consider two possible ways of producing transmitted and reflected ions: acceleration due to the solar wind electric field $\mathbf{E} = -\mathbf{V} \times \mathbf{B}$ tangent to the shock (Sonnerup 1969; Paschmann et al. 1980), or due to large amplitude waves present in the shock region.

We note that on the basis of our results, the acceleration mechanism has to produce a cut-off for the transmitted ions, this cut-off has to be at energies smaller than for the reflected ions. This cut-off has to move to higher energies as we go from upstream (foot of the shock) to downstream. The solar wind electric field acceleration could provide some of these features, but, on the other hand, it is difficult to understand the behaviour of the cut-off energy when going from the foot, through the shock, downstream, in terms of acceleration due to an electric field tangent to the shock. Acceleration due to waves must in any case be present in the foreshock region, producing diffuse ions with energies higher than the reflected ones.

Acknowledgements. We are very grateful to C.T. Russell of UCLA for providing us with unpublished ISEE magnetic field data. We are also grateful for the involvement of a number of staff of IPS-CNR, Frascati in the EGD plasma experiment.

References

Asbridge, J.R., Bame, S.J., Strong, I.B.: Outward flow of protons from Earth's bow shock. J. Geophys. Res. **73**, 5777–5789 (1968)

Bame, S.J., Adbridge, J.R., Feldman, W.C., Cosling, J.T., Paschmann, G., Schopke, N.: Deceleration of the solar wind upstream from the Earth's bow shock and the origin of diffuse upstream ions. J. Geophys. Res. **85**, 2981–2990 (1980)

Bonifazi, C., Egidi, A., Moreno, G., Orsini, S.: Backstreaming ions outside the Earth's bow shock and their interaction with the solar wind. J. Geophys. Res. **85**, 3461–3472 (1980)

Bonifazi, G., Cerulli-Irelli, P., Egidi, A., Formisano, V., Moreno, G.: The EGD positive ion experiment on the ISEE-B satellite. IEEE Trans. Geoscience Elect. **GE-16** 243–247 (1978)

Bonifazi, G., Moreno, G.: Reflected and Diffuse ions backstreaming from the Earth's bow shock: 2. Origin. J. Geophys. Res. **86**, 4405–4413 (1981)

Fairfield, D.H.: Bow shock associated waves observed in the far upstream interplanetary medium. J. Geophys. Res. **74**, 3451–3465 (1969)

Formisano, V.: The physics of the Earth's collisionless shock wave. J. Phys. **38**, C6, 65–88 (1977)

Formisano, V., Hedgecock, P.C.: Solar wind interaction with the Earth's magnetic field. III) On the Earth's bow shock structure. J. Geophys. Res. **78**, 3745–3760 (1973a)

Formisano, V., Hedgecock, P.C.: On the turbulent bow shock structure. J. Geophys. Res. **78**, 6522–6534 (1973b)

Formisano, V., Orsini, S., Bonifazi, C., Egidi, A., Moreno, G.: High time resolution observations of the solar wind in the Earth's foreshock region. Geophys. Res. Lett. **7**, 385–388 (1980)

Formisano, V., Amata, E.: Solar wind interaction with the Earth's magnetic field. 4-Preshock perturbation of the solar wind. J Geophys. Res. **81**, 3907–3912 (1976)

Gosling, J.T., Asbridge, J.R., Bame, S.J., Paschmann, G., Sckopke, N.: Observations of two distinct populations of bow shock ions in the upstream solar wind. Geophys. Res. Lett. **5**, 957–961 (1978)

Greenstadt, E.W.: The upstream escape of energized solar wind protons from the bow shock; in "The Magnetospheres of the Earth and Jupiter" ed. by V Formisano, Reidel Pub. Co. Dordrecht, Holland, 3–19 (1975)

Greenstadt, E.W., Russell, C.T., Hoppe, M.: Magnetic field orientation and suprathermal ion streams in the Earth's foreshock. J. Geophys. Res. **85**, 3473–3479 (1980)

King, J.H.: "Interplanetary medium data book Supplement 1" NASA NSSDC/WDC-A-R & S 79-08

Montgomery, M.D., Asbridge, J.R., Bame, S.J.: "Vela 4 plasma measurement observations near the Eaarth's bow shock" J. Geophys. Res. **75**, 1217–1230 (1970)

Paschmann, G., Sckopke, N., Bame, S.J., Asbridge, J.R., Gosling, J.T., Russell, C.T., Greenstadt, E.W.: Association of low frequency waves with suprathermal ions in the upstream solar wind. Geophys. Res. Lett. **6**, 209–212 (1979)

Paschmann, G., Sckopke, N., Asbridge, J.R., Bame, S.J., Gosling, J.T.: Energization of solar wind ions by reflection from the Earth's bow shock. J. Geophys. Res. **85**, 4689–4694 (1980)

Russell, C.T., Greenstadt, E.W.: Initial ISEE magnetometer results: shock observation. Space Sci. Rev. **23**, 3–37 (1979)

Sonnerup, B.V.Ö.: Acceleration of particles reflected at a shock front. J. Geophys. Res. **74**, 1301–1303 (1969)

Received January 22, 1981; Revised Version September 9, 1981
Accepted September 22, 1981